Fast qubit initialization in a superconducting circuit

Tianqi Huang(黄天棋), Wen Zheng(郑文), Shuqing Song(宋树清), Yuqian Dong(董煜倩), Xiaopei Yang(杨晓沛), Zhikun Han(韩志坤), Dong Lan(兰栋), and Xinsheng Tan(谭新生)

Citation: Chin. Phys. B, 2021, 30 (**7**): 070310. DOI: 10.1088/1674-1056/abff2b
Journal homepage: http://cpb.iphy.ac.cn; http://iopscience.iop.org/cpb

What follows is a list of articles you may be interested in

Improving the purity of heralded single-photon sources through spontaneous parametric down-conversion process

Jing Wang(王静), Chun-Hui Zhang(张春辉), Jing-Yang Liu(刘靖阳), Xue-Rui Qian(钱雪瑞), Jian Li(李剑), and Qin Wang(王琴)

Chin. Phys. B, 2021, 30 (**7**): 070304. DOI: 10.1088/1674-1056/abfb5c

Quantum computation and error correction based on continuous variable cluster states

Shuhong Hao(郝树宏), Xiaowei Deng(邓晓玮), Yang Liu(刘阳), Xiaolong Su(苏晓龙), Changde Xie(谢常德), and Kunchi Peng(彭堃墀)

Chin. Phys. B, 2021, 30 (**6**): 060312. DOI: 10.1088/1674-1056/abeb0a

Continuous-variable quantum key distribution based on photon addition operation

Xiao-Ting Chen(陈小婷), Lu-Ping Zhang(张露萍), Shou-Kang Chang(常守康), Huan Zhang(张欢), and Li-Yun Hu(胡利云)

Chin. Phys. B, 2021, 30 (**6**): 060304. DOI: 10.1088/1674-1056/abd931

Controlled quantum teleportation of an unknown single-qutrit state in noisy channels with memory

Shexiang Jiang(蒋社想), Bao Zhao(赵宝), and Xingzhu Liang(梁兴柱)

Chin. Phys. B, 2021, 30 (**6**): 060303. DOI: 10.1088/1674-1056/abea95

Detection efficiency characteristics of free-running InGaAs/InP single photon detector using passive quenching active reset IC

Fu Zheng(郑福), Chao Wang(王超), Zhi-Bin Sun(孙志斌), Guang-Jie Zhai(翟光杰)

Chin. Phys. B, 2016, 25 (**1**): 010306. DOI: 10.1088/1674-1056/25/1/010306

SPECIAL TOPIC — Quantum computation and quantum simulation

Fast qubit initialization in a superconducting circuit*

Tianqi Huang(黄天棋), Wen Zheng(郑文), Shuqing Song(宋树清), Yuqian Dong(董煜倩), Xiaopei Yang(杨晓沛), Zhikun Han(韩志坤), Dong Lan(兰栋), and Xinsheng Tan(谭新生)†

National Laboratory of Solid State Microstructures, School of Physics, Nanjing University, Nanjing 210093, *China*

(Received 23 March 2021; revised manuscript received 28 April 2021; accepted manuscript online 8 May 2021)

We demonstrate an active reset protocol in a superconducting quantum circuit. The thermal population on the excited state of a transmon qubit is reduced through driving the transitions between the qubit and an ancillary qubit. Furthermore, we investigate the efficiency of this approach at different temperatures. The result shows that population in the first excited state can be dropped from 7% to 2.55% in 27 ns at 30 mK. The efficiency improves as the temperature increases. Compared to other schemes, our proposal alleviates the requirements for measurement procedure and equipment. With the increase of qubit integration, the fast reset technique holds the promise of improving the fidelity of quantum control.

Keywords: active reset, quantum cooling, thermal population

PACS: 03.67.−a, 12.20.−m, 85.25.−j **DOI:** 10.1088/1674-1056/abff2b

1. Introduction

Quantum computation calls for high fidelity operation, which requires precise state preparation.[1–3] Instead of qubit initialization by passively waiting,[4] active reset can rapidly implement the preparation of the qubit system, increasing the experiment repetition rate. Meanwhile, by eliminating residual populations in excited states, the qubit can be thermally refrigerated, thus leading to fidelity improvement and decoherence suppression. Moreover, the active reset has indispensable applications in quantum error correction code,[5] where reusable ancillary qubits are essential.

Previously, there are several routines of active reset, one is measurement-based, such as post-select[6] and herald,[7] which reveals to be non-deterministic. Moreover, readout fidelity sets the limitation to reset performance due to the back action involved in measurement. A tempting improvement is feedback,[8–10] where iterative closed-loop control is performed by injecting π pulse triggered conditioning the outcome of the consecutive measurement. However, this method carries the drawbacks like relatively long latency (several hundred nanoseconds) and requirements for high-speed digits.

Apart from the above mentioned methods, alternative approaches like frequency detuning[11–14] and microwave driving[13–18] circumvent the requirement for high fidelity measurement. A primary idea rests in the latter involves dissipative environments engineering, such as reservoirs typically cooler than superconducting qubits, Purcell-filtered resonator,[12] quantum-circuit refrigerator,[19,20] and low-quality-factor cavity.[15–18,21] Nevertheless, with ancillary circuit elements introduced, this may cause the consumption of on-chip space and complex design of processor layout.

In this paper, we demonstrate a reset protocol in the platform of superconducting quantum circuit. Initially there is residual thermal population in the excited state of a target qubit (labeled as Q_a). We drive the target qubit and transfer the unwanted thermal population to an ancillary qubit, which is denoted as Q_b. Thus, the thermal population will be relocated from the computational space to the auxiliary levels. After tuning Q_b to the avoid-crossing point, a SWAP operation results in the cooling effect of the qubit. We characterize our approach at different temperatures and obtain the effective temperatures from fitting Dirac–Fermi statistics, which suggests that the qubit system can be effectively cooled after reset, thus performance improvement will be expected. Comparing to the current methods, our approach is fast and easy to implement. With the further increase of the operation fidelity, this technique provides a useful tool for scalable quantum processing.

2. Experiment method

In our experiment, the sample consists of six transmons, which are in an array with nearest-neighbor coupling through static capacitor (Fig. 1(c)). Each qubit is readout with an individual $\lambda/4$ coplanar resonator which is coupled to the transmission line on the sample. The chip is mounted in a dilution refrigerator with a temperature around 30 mK. Each qubit can be driven *in situ* by microwave signal (XY), and biased by inserting DC currents into flux lines (Z). The reflected signals from the resonators will be transported through co-axial lines and amplified by a HEMT amplifier, finally collected by the analog-to-digital converter. Without loss of generality, we

*Project supported by the National Key R&D Program of China (Grant No. 2016YFA0301802), the National Natural Science Foundation of China (Grant Nos. 61521001, 11474153, and 11890704), and the Key R/D Program of Guangdong Province, China (Grant No. 2018B030326001).

†Corresponding author. E-mail: txs.nju@gmail.com

initialize the target qubit (Q_a) via an ancillary qubit (Q_b) to demonstrate our scheme. The system Hamiltonian can be written as

$$\frac{\hat{H}}{\hbar} = \omega_a\sigma_a^\dagger\sigma_a + \omega_b\sigma_b^\dagger\sigma_b + \alpha_a\sigma_a^\dagger\sigma_a^\dagger\sigma_a\sigma_a + \alpha_b\sigma_b^\dagger\sigma_b^\dagger\sigma_b\sigma_b + J\left(\sigma_a^\dagger\sigma_b + \sigma_a\sigma_b^\dagger\right), \quad (1)$$

where ω_a (ω_b), $\sigma_a^\dagger$ ($\sigma_b^\dagger$), σ_a (σ_b), and α_a (α_b) are the qubit frequency, generation operator, annihilation operator, and anharmonicity of Q_a (Q_b), respectively. J is the coupling strength between qubits. System parameters were measured to be $\omega_{01}/2\pi = 4.925\,(5.8)$ GHz, $\omega_{12}/2\pi = 4.645\,(5.531)$ GHz, $\alpha/2\pi = 280\,(268.6)$ MHz, $T_1 = 16.5\,(21.6)$ μs, $T_2^* = 3.5(2.9)$ μs for Q_a (Q_b).

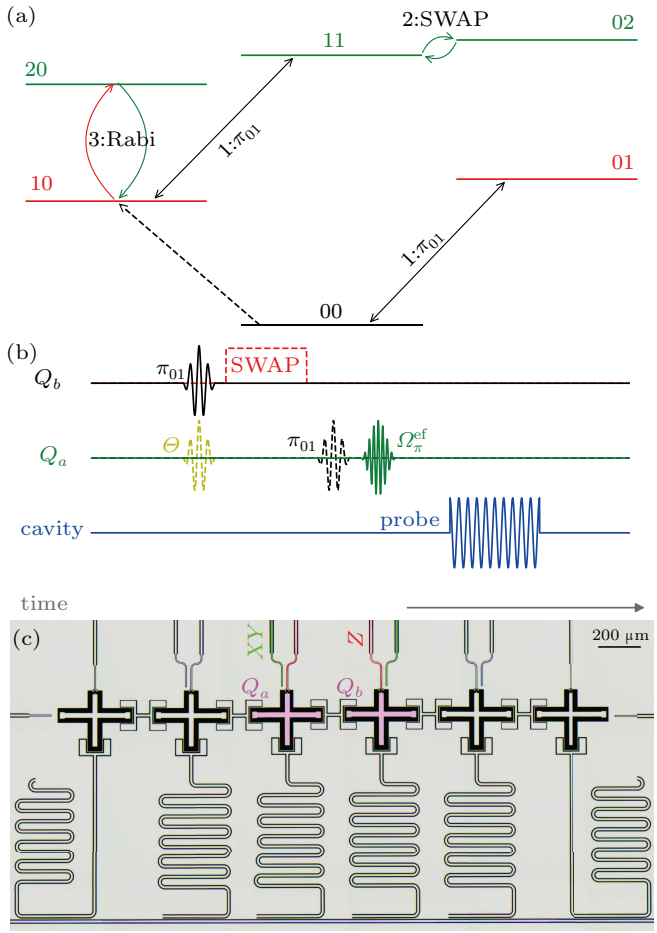

Fig. 1. (a) Diagram illustrating the principle of our protocol with Q_a and Q_b. Step 1, a π_{01} pulse corresponding to the transition frequency in the $\{|0_b\rangle, |1_b\rangle\}$ subspace of Q_b. Step 2, a tailored square pulse sented through flux bias line, whose voltage and duration are finely tuned to perform a full SWAP gate at the avoid-crossing point of $|1_a1_b\rangle \leftrightarrow |0_a2_b\rangle$. Step 3, a Rabi oscillation pulse Ω_π^{12} driving qubit evolution in $\{|1_a\rangle, |2_a\rangle\}$ subspace, following a π pulse flipping the $|0_a\rangle$ and $|1_a\rangle$ states of Q_a. (b) Pulse sequence versus time. The yellow pulse is aimed to prepare Q_a to an arbitrary superposition state in the $\{|0_a\rangle, |1_a\rangle\}$ subspace. A probe pulse is produced at the end of every round. (c) Blue (green, red, and magenta) color represents transmission line (drive line, flux line, and transmons).

Our scheme is divided into two steps, as illustrated in Fig. 1(b). First, we promote a π_{01} pulse to Q_b, in order to flip the populations between $|0_b\rangle$ and $|1_b\rangle$ states, which can be expressed as a transformation matrix $\hat{U}_{b\pi} = \sum_i(|i_a1_b\rangle\langle i_a0_b| + |i_a0_b\rangle\langle i_a1_b|)$. Second, a flux pulse is applied to Q_b to ramp it approaching the avoid-crossing point of $|1_a1_b\rangle \leftrightarrow |0_a2_b\rangle$ transition, inducing vacuum-Rabi oscillations between two qubits. After fixed flux pulse duration (i.e., 27 ns), a full SWAP operation $\hat{U}_{\rm SWAP} = |0_a2_b\rangle\langle 1_a1_b| + |1_a1_b\rangle\langle 0_a2_b|$ is conducted, resulting in population reversal between $|1_a1_b\rangle$ and $|0_a2_b\rangle$.

By tracing out the degree of freedom of the ancillary qubit Q_b, one can obtain the state matrix of the target qubit Q_a. As $\hat{\rho}_a = (P_{00} + P_{01} + P_{10})|0_a\rangle\langle 0_a| + P_{11}|1_a\rangle\langle 1_a|$. The population in the excited state is deduced as P_{11}. Nevertheless, this figure merely gives an optimal estimate which can hardly be reached in this experiment owing to the drawbacks in our system, and we will give an analysis latter.

Normally, we obtain the population of each energy levels from the measured amplitude of the signal, which can be written as

$$V_{\rm m} = \Sigma_i\alpha_iP_i, \quad (2)$$

where P_i is the population at $|i\rangle$ and α_i is the ideal voltage measured when the qubit is at $|i\rangle$. Notice that normally α_i is calibrated, and we solve P_i from the equation above. However, in this experiment, we can not obtain the α_i directly, due to the noise of our instruments. Here we utilize a routine to obtain P_i, in which an additional step is introduced. We drive a Rabi oscillation of Q_a between $|1_a\rangle$ and $|2_a\rangle$ states by an Ω_π^{12} pulse (green solid line). The outcome signal can be fitted to a sinusoidal envelope $A_{1(0)}\cos(\theta)$. A_0 and A_1 correspond to different situations whether Q_a is prepared to $|0_a\rangle$ or $|1_a\rangle$ previously (black dash line), whose expression is given as

$$A_{1(0)} = V_2 - V_1 = (\alpha_2 - \alpha_1)(P_{1(0)} - P_2). \quad (3)$$

Since $P_2 \ll P_1$, we can deduce the spurious excited populations P_1, as below:

$$P_1 = A_1/(A_1 + A_0). \quad (4)$$

3. Results and discussion

Considerring the fact that the fringe of Rabi oscillations is proportional to P_1, one can characterize the residual thermal population by Rabi oscillation. We obtained that the initial equilibrium P_1 of Q_a is around 7% at 30 mK. After reset, P_1 achieved 2.55%. To amplify the cooling effect and investigate the efficiency changing with the temperature, we then increased the temperature of the cold plate of the dilution refrigerator. The Rabi oscillations at different temperatures (50 mK, 100 mK, 150 mK) are plotted in Fig. 2. Figure 2(a) corresponds to reset Q_a. Only three periods of Rabi oscillations are shown, whose amplitudes are fitted by the standard Rabi model (solid and dash lines), from which we can calculate the spurious thermal populations to be (0.1096, 0.1385, 0.1859) and (0.0309, 0.0445, 0.0786) before and after the reset. As the temperature

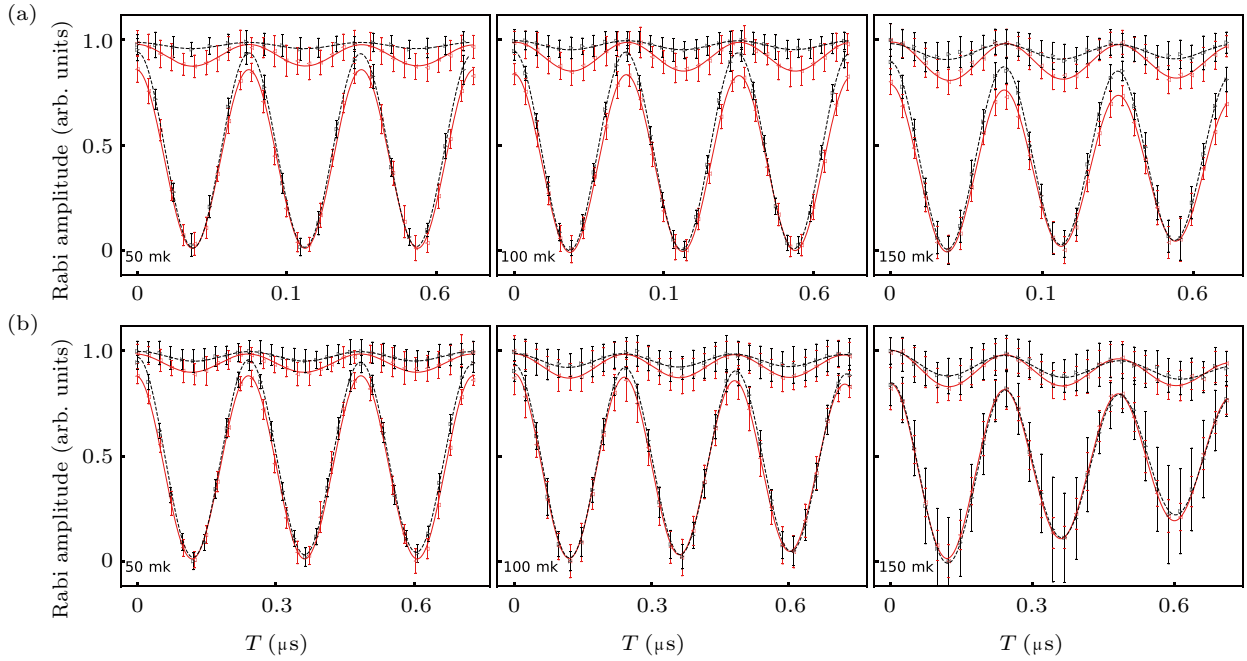

Fig. 2. (a) Rabi oscillations of Q_a at different temperatures (50 mK, 100 mK, 150 mK). X (Y) axis is the Rabi evolution time (normalized Rabi amplitude). Red (black) dots along with error bars depict results without (with) reset. Solid (dash) line is fitted to the standard Rabi model, from which we can calculate the spurious thermal populations to be (0.1096, 0.1385, 0.1859) and (0.0309, 0.0445, 0.0786) before and after the reset. (b) Reset outcomes of Q_b. The spurious thermal populations are calculated to be (0.0907, 0.1153, 0.1655) and (0.0464, 0.0688, 0.1146) before and after the reset.

rise, more quasi-particles will be invoked,[22] leading to the deterioration of remnant thermal populations. The efficiency increases. Figure 2(b) shows the outcomes related to reset Q_b using Q_a. Similarly, the spurious thermal populations are (0.0907, 0.1153, 0.1655) and (0.0464, 0.0688, 0.1146) before and after the reset. Switching the roles of the qubits produces a variation in the reset performance, which arises from the environmental differences experienced by Q_a and Q_b. When climbing up to 150 mK, the lines become skewed owing to the reduced dephasing time.

To characterize the efficiency for different initial states, we prepare Q_a at a superposition state, as shown in Fig. 3(a). We demonstrate the reset efficiency η to be $(P_1 - P_1')/P_1$, a figure comparing the relative change of P_1 before and after the reset, which can be referred in the inset. In the worst case, all populations are initialized in $|1\rangle$ ($\Theta = \pi$), the reset operation becomes equivalent to a single π flip, thus η is almost zero. While prepared at $|0\rangle$, the efficiency is around 100% theoretically.

It is worth noting that the deviation of experiment results from theory can be primarily attributed to the limited SWAP gate fidelity, which is measured to be 98%. The distortions in flux pulses are unavoidable, owing to the limited bandwidth in digital devices and lines. Previously added flux pulses and crosstalk with other qubits also bring error. In recent publications, several groups have enhanced two-qubit gate fidelity to over 99.6%,[2,23] which opens up an opportunity to display the advantage of our method by carrying out a high fidelity SWAP gate. We investigate that through perfect pulse parameters,

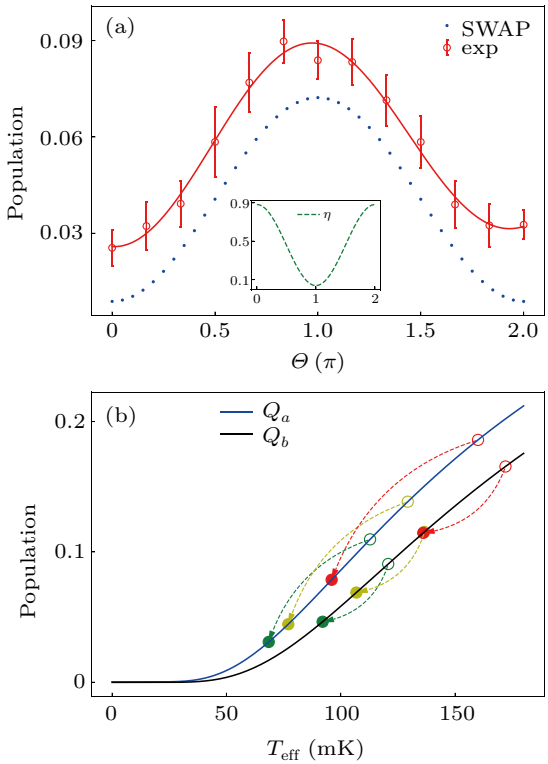

Fig. 3. (a) The chart illustrates the reset results for Q_a from arbitrary superposition states at 30 mK (red dots along with error bars displaying the standard deviations). The horizontal axis corresponds to evolve along the longitude of the Bloch sphere for one period. The solid line is fitted to a Rabi model. A minimum P_1 reads 2.55% at $\Theta = 0$, representing the residual thermal population after reset. The dot lines are the simulated results using the Qutip package. The inset gives an example of reset efficiency η. When the qubit is initialized to $|0\rangle$ ($|1\rangle$), η reaches the maximum (minimum). (b) Using the statistics from Fig. 2, one can calculate the effective temperatures of the qubit with Dirac–Fermi distribution. $T_{\rm eff}$ differs a bit for Q_a and Q_b, due to the different environments experienced by the qubits. Here, different colors (green, yellow, red) correspond to temperatures at 50 mK, 100 mK, 150 mK, respectively.

the reset performance can be improved substantially, by eliminating the thermal population to less than 1%, thus fulfilling the request for error correction.

From another perspective of view, we further derive the effective temperatures T_{eff} of the qubits using the statistics from Fig. 2 according to Dirac–Fermi distribution (Fig. 3(b)). Due to the difference in the environments experienced by the qubits, T_{eff} differs a bit for Q_a and Q_b. Specifically, at different temperatures (50 mK, 100 mK, 150 mK), Q_a is cooled from (112.83 mK, 129.31 mK, 160.04 mK) to (68.5 mK, 77.07 mK, 96.02 mK), and Q_b from (120.75 mK, 136.60 mK, 172.05 mK) to (92.08 mK, 106.84 mK, 136.1 mK).

4. Conclusion

We propose and realize an active reset protocol in cQED, showing a potential to eliminate residual thermal population in 27 ns, which is faster than the results reported before. This scheme calls for neither feedback nor dissipative environment, only a spare qubit is required. Besides, it is general and can be easily transported to other architectures, like trapped-ion,[24] NV-center,[25] quantum dots,[26] etc. Since amplifying the signal strength can significantly improve the accuracy and speed of state discrimination, one can further improve the efficiency of reset by using a JPA to readout the qubit.

References

[1] Arute F, Arya K, Babbush R, *et al.* 2020 *Science* **369** 1084
[2] Arute F, Arya K, Babbush R, *et al.* 2019 *Nature* **574** 505
[3] Blais A, Girvin S M and Oliver W D 2020 *Nat. Phys.* **16** 247
[4] Ladd T D, Jelezko F, Laflamme R, Nakamura Y, Monroe C and O'Brien J L 2010 *Nature* **464** 45
[5] Barends R, Kelly J, Megrant A, *et al.* 2014 *Nature* **508** 500
[6] Ristè D, Van Leeuwen J G, Ku H S, Lehnert K W and DiCarlo L 2012 *Phys. Rev. Lett.* **109** 050507
[7] Johnson J E, MacKlin C, Slichter D H, Vijay R, Weingarten E B, Clarke J and Siddiqi I 2012 *Phys. Rev. Lett.* **109** 050506
[8] Campagne-Ibarcq P, Flurin E, Roch N, Darson D, Morfin P, Mirrahimi M, Devoret M H, Mallet F and Huard B 2013 *Phys. Rev. X* **3** 021008
[9] Ristè D, Bultink C C, Lehnert K W and DiCarlo L 2012 *Phys. Rev. Lett.* **109** 240502
[10] Salathè Y, Kurpiers P, Karg T, Lang C, Andersen C K, Akin A, Krinner S, Eichler C and Wallraff A 2018 *Phys. Rev. Appl.* **9** 034011
[11] Mariantoni M, Wang H, Yamamoto T, *et al.* 2011 *Science* **334** 61
[12] Reed M D, Johnson B R, Houck A A, DiCarlo L, Chow J M, Schuster D I, Frunzio L and Schoelkopf R J 2010 *Appl. Phys. Lett.* **96** 203110
[13] Grajcar M, Van Der Ploeg S H, Izmalkov A, Il'ichev E, Meyer H G, Fedorov A, Shnirman A and Schön G 2008 *Nat. Phys.* **4** 612
[14] Valenzuela S O, Oliver W D, Berns D M, Berggren K K, Levitov L S and Orlando T P 2006 *Science* **314** 1589
[15] Egger D J, Werninghaus M, Ganzhorn M, Salis G, Fuhrer A, Müller P and Filipp S 2018 *Phys. Rev. Appl.* **10** 044030
[16] Magnard P, Kurpiers P, Royer B, *et al.* 2018 *Phys. Rev. Lett.* **121** 060502
[17] Basilewitsch D, Schmidt R, Sugny D, Maniscalco S and Koch C P 2017 *New J. Phys.* **19** 113042
[18] Geerlings K, Leghtas Z, Pop I M, Shankar S, Frun-zio L, Schoelkopf R J, Mirrahimi M and Devoret M H 2013 *Phys. Rev. Lett.* **110** 120501
[19] Tan K Y, Partanen M, Lake R E, Govenius J, Ma-suda S and Möttönen M 2017 *Nat. Commun.* **8** 15189
[20] Tuorila J, Stockburger J, Ala-Nissila T, Ankerhold J and Möttönen M 2019 *Phys. Rev. Res.* **1** 13004
[21] Tuorila J, Partanen M, Ala-Nissila T and Möttönen M 2017 *npj Quantum Inf.* **3** 27
[22] Jin X Y, Kamal A, Sears A P, *et al.* 2015 *Phys. Rev. Lett.* **114** 240501
[23] Sung Y, Ding L, Braumüller J, *et al.* 2021 *Phys. Rev. X* **11** 021058
[24] Häffner H, Hänsel W, Roos C F, *et al.* 2005 *Nature* **438** 643
[25] Kubo Y, Ong F R, Bertet P, *et al.* 2010 *Phys. Rev. Lett.* **105** 140502
[26] Loss D and DiVincenzo D P 1998 *Phys. Rev. A* **57** 120